Synthesis and Evaluation of Ion Recognition Properties of Schiff base Appended on Hydroxyphenyl-benzimidazole

A

Dissertation report submitted

in the partial fulfillment of the requirement of the degree of

MASTER OF SCIENCE
IN
CHEMISTRY

BY
Anju Nalini Garg
(Roll No. 302102004)

Under the Supervision of
Dr. Priya Vashisht
Assistant Professor

Under the Supervision of
Dr. Vijay Luxami
Professor

SCHOOL OF CHEMISTRY AND BIOCHEMISTRY
THAPAR INSTITUTE OF ENGINEERING AND TECHNOLOGY
Patiala-147004 Punjab, India
July, 2023

CANDIDATE DECLARATION

I hereby declare that the work being presented in thesis entitled **"Synthesis and Evaluation of Ion Recognition Properties of Schiff base Appended on Hydroxyphenyl-benzimidazole** " is submitted in partial fulfillment of requirements for the award of degree of **Masters of Science in Chemistry,** submitted in the **School of Chemistry and Biochemistry, Thapar Institute of Engineering and Technology, Patiala** is a record of my own work carried out under the guidance and supervision of **Dr. Vijay Luxami** and **Dr. Priya Vashisht** from the period of January 2023 to June 2023. I have not submitted the matter embodied in the thesis for award of any other degree.

Signature of Candidate
Place: Patiala, Punjab
Date: 29-07-2023

Anju Nalini Garg
(302102004)

CERTIFICATE

This is to certify that the thesis entitled "**Synthesis and Evaluation of Ion Recognition Properties of Schiff base Appended on Hydroxyphenyl-benzimidazole**" submitted by **Ms. Anju Nalini Garg (Roll no. 302102004)** in the partial fulfillment of the requirement for the degree of **Masters of Science in Chemistry**, from Thapar Institute of Engineering and Technology, Patiala is a bonafide piece of work carried out under the guidance and supervision of **Dr. Vijay Luxami**, Professor, School of Chemistry and Biochemistry and **Dr. Priya Vashisht**, Assistant Professor, School of Chemistry and Biochemistry, Thapar Institute of Engineering and Technology, Patiala and no part has been submitted for the award for any other degree in any other university

This is to certify the above statement made by student cornered is correct and true to the best of my knowledge.

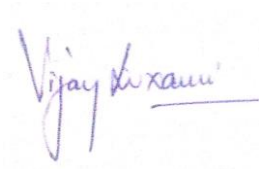

Dr. Vijay Luxami
Professor
School of Chemistry and Biochemistry
Thapar Institute of Engineering and Technology, Patiala

Dr. Priya Vashisht
Assistant Professor
School of Chemistry and Biochemistry
Thapar Institute of Engineering and Technology, Patiala

ACKNOWLEDGEMENT

First of all, I would want to offer my sincere appreciation to the Supreme Almighty for protecting me and keeping me comfortable while I conducted my study. I'm grateful to **Dr. Satnam Singh, Professor and Head of the School of Chemistry and Biochemistry, T.I.E.T, Patiala (Punjab)** for providing me with this great opportunity and letting me access a variety of the department's resources.

I am really grateful to **Dr. Vijay Luxami**, Professor and **Dr. Priya Vashisht**, Assistant Professor of **School of Chemistry and Biochemistry, T.I.E.T, Patiala, Punjab** for their worthy guidance, valuable suggestions, inspiration and leadership. They provided me with a lot of assistance during my investigation, from basic facilities to advice. I can't express how grateful I am for their advice and assistance.

I would like to thank **Dr. Davinder Kumar**, P.G. coordinator, for his continuous support and my sincere gratitude to **Aastha Palta** for being there for me during my study. I appreciate that she corrected me every time I made a mistake while working on this assignment. Her friendliness made it easier for me to finish my job. Our communication has proven to be quite beneficial.

Working with PhD students **Rekha Thakur, Rohini Gupta, Saurabh Gupta, Palak Sharma, Sonia Wadhwa, Anmol Jain, Tanya and Shifali** has been a really positive experience for me, and I am grateful to them for their assistance. My whole hearted thanks to **Mr. Chander Thakur** and **Mr. Hemant Kumar** and all other lab attendants for their valuable help and immense support. This work would not have been possible without my lab mates **Abhishek, Abhinav** and **Amrit** who made this trip enjoyable. Without the assistance of SAI labs at Thapar Institute of Engineering and Technology, Patiala, the majority of the findings in the thesis would not have been achievable.

In the presence of this project, there has been an important role of my father **Mr. Satpal Garg**, my mother **Mrs. Kiran Bala Garg** and my brothers and sisters and I am grateful to them for their unwavering love, encouragement, and support of me in every way.

Date: 29-07-2023 **Anju Nalini Garg**

Abstract

A simple, tailor made, novel chemosensor **3** based on benzimidazole incorporating 2-Hydroxy-1-napthaldehyde was designed and synthesized that showed intramolecular charge transfer (ICT) and Aggregation induced emission (AIE) phenomenon. The photophysical properties of chemosensor **3** were evaluated via colorimetric, UV-vis and fluorescence techniques. Chemosensor **3** displayed absorption band at 355 nm while an emission band at 450 nm and 530 nm (20 µM, H_2O). Amongst all the tested anions, the visible color change from dark yellow to light yellow was observed only with CN^- addition. Moreover, under UV light, the blue fluorescence of chemosensor **3** was enhanced only in the presence of CN^- ion. From the photophysical behavior of chemosensor **3**, it was examined that the chemosensor **3** exhibited selective behavior towards CN^- ion. The emission bands at 450 nm and 530 nm exhibited blue shift of 40 nm and 120 nm respectively. The fluorescence of **3** was enhanced appreciably with CN^- addition and the increased fluorescence was not interfered with any of the other competent ions. Significantly, the detection limit of chemosensor **3** for CN^- was evaluated to be 3.3×10^{-7} M with the binding constant value of 2×10^{-3} M^{-1}. Chemosensor **3** formed 1:1 complex with CN^- ion as suggested by Job's plot method.

Table of Content

LIST OF FIGURES

ABBREVIATIONS

CH_3COO^-	Acetate anion
CH_3CN	Acetonitrile
AIE	Aggregation Induced emission
Br^-	Bromide ions
Cl^-	Chloride ion
CN^-	Cyanide ion
DLS	Dynamic light scattering
$H_2PO_4^-$	Dihydrogen Phosphate Anion
DMSO	Dimethyl sulfoxide
DCP	Diethyl chlorophosphate
$CDCl_3$	Deuterochloroform
ESICT	Excited state intramolecular charge transfer
ESIPT	Excited State Intramolecular Proton Transfer
F^-	Fluoride ions
FRET	Fluorescence resonance energy transfer
gm	Gram
HSO_4^-	Hydrogen Sulfate anion
HPLC	High-Performance liquid chromatography
H- bonding	Hydrogen bonding
HRMS	High-resolution mass spectrometry
IR	Infrared spectroscopy
I^-	Iodine
ICT	Intramolecular Charge Transfer
IUPAC	International Union of Pure and Applied Chemistry
LOD	Limit of Detection
mg	Milligram
mmol	Mili molar
µM	Micromolar
NO_3^-	Nitrate anion

NMR	Nuclear magnetic resonance
nm	Nano meter
ns	Nano second
$P_2O_7^{4-}$	Pyrophosphate
PET	Photo-induced electron transfer
ppm	Parts per million
TLC	Thin Layer Chromatography
SCN^-	Thiocyanate
THF	Tetrahydrofuran
TGA	Thermogravimetric analysis
WHO	World health organization

CHAPTER 1

INTRODUCTION AND LITERATURE REVIEW

1.1.Introduction

Supramolecular chemistry has created the way for an exciting and active field of research that is focused on the development of chemosensors, which can well detect environmentally and biologically relevant ions [1]. These chemosensors have the capacity to bind to the target analyte in a selective and reversible manner, causing precise changes to some of system characteristics such as redox potential, absorbance, and fluorescence [2]. Due to excellent sensitivity, selectivity and non-invasive nature, fluorescence-based methods have been used in a wide range for both academic and industrial sectors. Small-molecule fluorescent chemosensors, owing to their easy design and synthesis, act as the basic components for sensing and imaging applications, hence the key agents to these techniques [3]. The use of Schiff bases as highly selective and sensitive sensing materials have gained considerable attention as novel fluorescent chemosensors that can identify and monitor ions [4].

Schiff bases, commonly referred to as imines or azomethines are crucial in the development of fluorescent chemosensors because of their facile synthesis and remarkable ability to form stable complexes with ions [5]. The ability of Schiff bases to detect and monitor ions in diverse biological, environmental, and chemical processes was mainly due to their ease of synthesis, solubility in common solvent and flexibility of structural changes [6]. Schiff bases besides being widely used in pharmaceuticals and agro-industrial industries, are also as used as the pigments, catalysts, organic synthesis intermediates and for metal ion sensing. In the recent past, synthesizing Schiff base fluorescent chemosensors has been of the utmost biological importance as a detection method for various anions [7].

Due to the recent rapid expansion of modern industries, anions have significantly contributed in pollution, posing a serious hazard to both human health and environment safety [8]. Many chemosensors have been developed over the recent years for the detection of different poisonous gases and pollutants, such as anions, organic dyes, and other harmful substances. The CN^- ion has emerged as the most hazardous and toxic in the environment amongst the different prevalent anions. Many industries involved in metallurgy, leather manufacturing, electroplating, and plastic synthesis, frequently employ cyanide ions (CN^-). Unfortunately, CN^- is released into the

environment as a result of its usage in these industries [9]. CN^- exposure can seriously harm a person's health, including their vision, endocrine system, heart and even central nervous system. Therefore, it is essential to recognize and detect CN^- ion for the safety of the human body and the environment. On the other hand, fluorescent chemosensors have attracted a lot of interest for CN^- ion detection in aqueous solution due to their high selectivity and sensitivity, low cost, quick response and low detection limits [9–10]. The techniques of photo-induced electron transfer (PET), intramolecular charge transfer (ICT), and fluorescence resonance energy transfer (FRET) along with other sensing mechanistic modes such as H-bonding and complexation have been identified as the possible methods for the detection of CN^- ion. [11].

In recent years, a wide variety of moieties have been used for the synthesis of fluorescent chemosensors, including benzimidazole, rhodamine, benzothiazole, coumarin, fluorescein, quinoline, naphthalimide, and 1, 10-phenanthroline. These moieties serve well for CN^- ion detection because they provide nitrogen and oxygen atoms which make easier coordination with CN^-. Due to their inherent fluorescent characteristics, benzimidazole derivatives from the above-mentioned moieties have attracted a lot of attention in the field of fluorescence-based chemosensors. This inherent fluorescent property increases the flexibility and adaptability of chemosensors based on benzimidazole derivatives. The hydroxyl and imine groups are added to the benzimidazole as particular binding sites to enable the use of hydrogen bonding interactions and nucleophilic addition mechanism, which makes it easier to detect CN^- ions. As a result, attempts to explore and develop benzimidazole derivatives as adaptable chemosensors for numerous applications have achieved great success in the fields of optical and chemical analysis [12, 13].

Therefore, the purpose and goal of this thesis was to develop innovative chemosensors based on Schiff bases and their complexes, specifically incorporating benzimidazole. The primary focus was to assess the binding and sensing capabilities of these chemosensors for CN^- ion that hold significant importance in biological and environmental context. The current study presents the synthesis and binding properties of benzimidazole appended novel Schiff base incorporating 2-hydroxy-1-napthaldehyde.

1.2.Literature Review

Kandemir et al. synthesized coumarin-thiazole based chemosensors **1a & 1b** for the detection of CN^- ions [14]. Using UV-vis and fluorescence spectrophotometers their photophysical studies were completed in six different solvents. Along with the detection of CN^-, chemosensors also demonstrated the detection of interfering anions such as F^-, AcO^-, and $H_2PO_4^-$ dissolved in water. Among these anions CN^- ion is extremely selective, which can be employed for colorimetric detection of chemosensors in aqueous solutions. The mechanism was studied using reversibility and ^1H NMR. Although calculated LOD values (0.17 µM and 0.27 µM) of chemosensors **1a & 1b** for CN^- ion in both DMSO and DMSO: H_2O (5:5) were found to be lower than WHO recommended value (2.7 µM), so chemosensors can be used to determine CN^- at lower concentrations. Moreover, the chemosensor had good thermal stability for their applications in electro-optic materials.

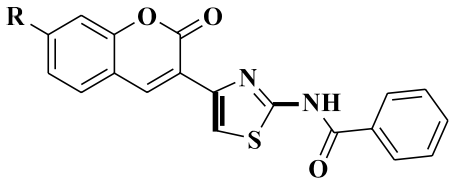

1(a) R:-H **1(b) R:-NEt_2**

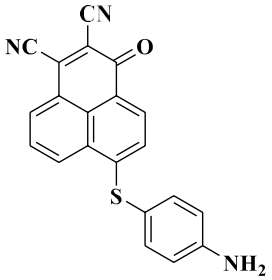

(2)

Mehta et al. synthesized chemosensor **2** based on phenalene dicarbonitrile that responded specifically to CN^- ions in both colorimetric and fluorescence detection [15]. On addition of CN^- ions, the chemosensor showed a noticeable change in both UV-Vis and fluorescence spectra. With the addition of CN^- ions, quenching occurred at 527 nm with the appearance of new band at 454 nm in the absorption spectra, whereas the intensity of emission band at 567 nm was enhanced with bright yellow emission. The sensor displayed binding constant value of 1.1×10^4 M^{-1} as determined using fluorescence titration, and was able to detect CN^- ions to as low as 5.5×10^{-8} M. The chemosensor could detect CN^- ions in industrial effluents and have been used in the formation of a 1-to-2 decoder.

Kumar et al. synthesized an imidazole-based chemosensor **3** containing hexamethylenetetramine and 2-(4, 5- diphenyl-1H-imidazol-2-yl) phenol that could detect CN^- both via colorimetric and fluorometric behavior in aqueous media [16]. The incremental addition of CN^- caused the color change from colorless to green with blue shifted emission band from 438 to 420 nm. In the pH range of 6-12, the chemosensor showed the detection limit of 7.87 nm with the binding ratio of 1:1. This mechanism explained the nucleophilic attack of CN^- ion on the dione-vinyl site, which enabled the intramolecular charge transfer (ICT) process.

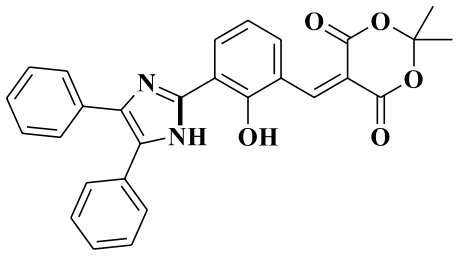

(3)

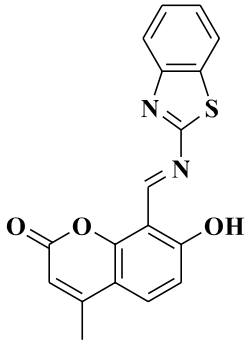

(4)

Ghosh et al. synthesized a Schiff base chemosensor **4** based upon Coumarinyl-Benzothiazolyl derivative characterized using various spectroscopic techniques [17]. Chemosensor **4** served as a "turn-on" type fluorescent chemosensor for CN^- in the DMSO solution. The binding constant of the chemosensor was found to be 0.696 x 10^4 M^{-1} with the detection limit of 0.75 µM towards CN^- ions using absorption and emission spectra. The sensing mechanism of chemosensor towards CN^- includes deprotonation of the -OH group and nucleophilic attack on the imine (-CH=N-) bond which was confirmed using ^{1}H- NMR titration. The chemosensor was tested on MDA-MB 231 cell line and MTT assay showed no up in toxicity till 100 µM.

Yao et al. synthesized an azine derived chemosensor **5** used for detecting the CN^- ion [18]. The chemosensor showed dual-channel behavior with high selectivity and sensitivity towards CN^- ion in aqueous media. The fluorescence quenched at 562 nm with a noticeable color shift from colorless to yellow with the addition of CN^-. The LOD was found to be 1.02×10^{-8} M calculated using fluorescence titration data of chemosensor to CN^-.

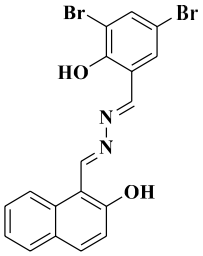

(5)

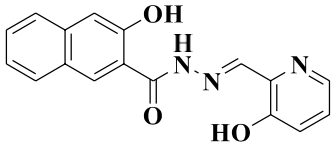

(6)

Liu et al. designed a "turn-off" fluorescent chemosensor **6** based on AIE active dual-channel chemosensor used specifically for the detection of CN^- ion in the DMSO solution [19]. With the incremental addition of CN^- ion a strong absorption peak at 329 nm was greatly reduced and accompanied by a new peak at 368 nm indicating red shift while emission intensity of peak at 482 nm was quenched appreciably. Moreover, the visible color change from colorless to yellow was also exhibited with CN^- addition. The binding ratio of chemosensor and CN^- was evaluated to be 1:2 using job's plot and the detection limit was found to be as low as 9.93 nM for the CN^- ion.

Song et al. developed cyanide detecting chemosensor **7** which showed ICT ON process [20]. The nucleophilic reaction of CN^- to sensor's C=C might be responsible for the identification of CN^- via breaking down of π-conjugation and hence preventing its ICT effect (ICT OFF). This led to both colorimetric and fluorometric responses of **7** towards CN^- ion. With a broad fluorescence emission of 595 nm and absorption peak of 450 nm, chemosensor exhibited the large stokes shift of 145 nm. The addition of CN^- ion to chemosensor led to fluorescence quenching with the visible color change from orange to colorless. Chemosensor displayed remarkable sensitivity to CN^- ion with a detection limit of 0.70 µM.

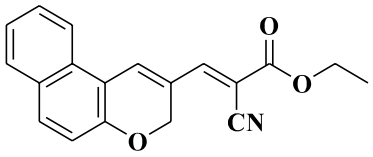

(7)

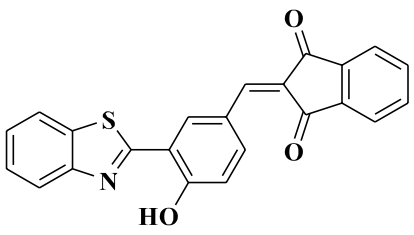

(8)

Jothi et al. designed fluorogenic chemosensor **8** based on benzimidazole and utilized it for the recognition of CN^- ion [21]. The sensor displayed a fluorescence emission band at 625 nm and two absorption bands at 300nm and 398 nm in CH_3CN/H_2O solution. When significant amount of CN^- ions were added to the solution a new absorption band was observed at 593 nm. Furthermore, due to the absence of the ICT process, the chemosensor displayed a blue shift in emission wavelength from 625 nm to 512 nm on binding with the CN^- ions. According to the job's plot, the binding ratio for CN^- ions to the chemosensor was found to be 1:1.

Hemalatha et al. developed a colorimetric Schiff base chemosensor **9** for the detection of CN^- ion [22]. The chemosensor showed high selectivity and sensitivity towards the CN^- ions over the other anions due to deprotonation and intramolecular charge transfer, with a color change from yellow to brown. Due to deprotonation, the chemosensor exhibited a red shift in the absorption band from 359 nm to 447 nm with the addition of the CN^- ions. The detection limit of the chemosensor towards CN^- ion was calculated to be 7.39×10^{-7} M using UV-vis titration data. The chemosensor was tested for its practical applicability using paper strips and cotton swabs.

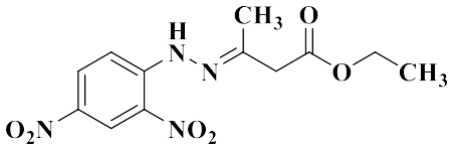

(9)

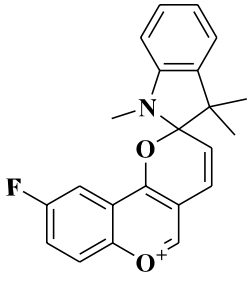

(10)

Maurya et al. synthesized an indolium based spiropyran chemosensor **10** which acted as the chromogenic and fluorogenic chemodosimeter for selective detection of CN^- ion [23]. The chemosensor exhibited π-π^* and n-π^* transition with weak emission intensity at 520 nm. In the absorption spectrum, the absorption bands at 242 and 381 nm decrease in intensity with the addition of CN^- ion accompanied by the color change from light green to yellow. However in the fluorescence spectra, the emission intensity of the band at 520 nm was enhanced leading to the non- fluorescent to fluorescent green color of the solution. The nucleophilic addition of CN^- via ring opening, which is related to a decrease in ICT chromone unit transition and emission amplification, specified the sensing mechanism. The binding ratio was found to be 1:1 with

detection limit of 57.9 nm and rate constant of 0.022 S^{-1} for the interface between chemosensor and CN^-

Ozdemir et al. synthesized a "turn-on" fluorescent chemosensor **11** using triphenylamine and phenanthroimidazole units [24]. The chemosensor showed absorption bands at 382 and 462 nm while weak fluorescence emission at 430 and 435 nm. With the addition of CN^- ion, the absorption band at 462 nm disappeared with the color change of solution from yellow to colorless while the emission intensity was enhanced, probably due to the π-conjugation and ICT effect to β-carbon of the dicyanovinyl moiety of chemosensor. The chemosensor displayed 5.36(log Ka) as the binding constant value calculated using Benesi-Hildebrand equation, and the detection limit was found to be 0.2 μM with binding ratio of chemosensor to anion is 1:1.

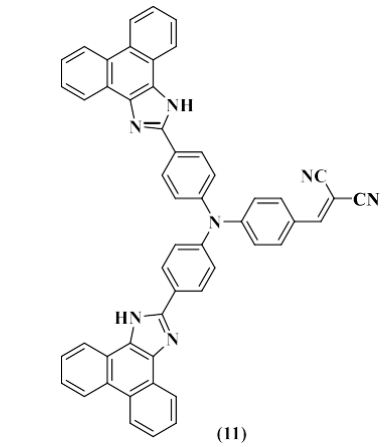

(11)

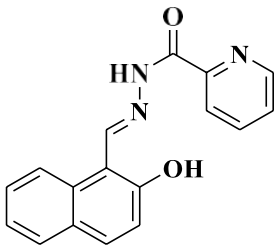

(12)

Dey et al. developed a Picolinohydrazide-naphthol as a Schiff base chemosensor **12** which is utilized for the sensitive and selective detection of CN^- ion in DMSO: H2O solution [25]. The chemosensor showed four absorption bands at 314, 328, 365 and 380 nm but decreased due to the formation of new band at 460 nm with the addition of CN^- ion. At pH 7.2, chemosensor showed the visual color change from colorless to yellow with LOD 7.08μM. The plausible mechanism behind the sensing behavior of chemosensor towards CN^- could be the deprotonation of naphthol -OH by CN^-, which was been verified using ^1H NMR titration and mass spectra, Job's plot supported the composition ratio of chemosensor to CN^- as 1:1, while the Benesi-Hildebrand plot reported the binding constant value of 1.5×10^4 M^{-1}.

Xue et al. designed and synthesized a ratiometric fluorescent chemosensor **13** based on the 1,4-dihydropyridine for the detection of CN^- ion in aqueous media [26]. The chemosensor displayed two absorption peaks at 400 nm and 650 nm. However, on addition of CN^- ion, a new absorption peak appeared at 542 nm with gradual color change of solution from red to green. The emission intensity of the band at 700 nm was quenched with simultaneous appearance of peak at 440 nm, with the color change from blue to red with the addition of CN^- ion to chemosensor. The chemosensor displayed a very significant (260 nm) shift in the fluorescence emission peak. The LOD value was found to be 2.74×10^{-7} M. The process occurred as CN^- showed nucleophilic attack on the indole group of the chemosensor which inhibited the intramolecular charge transfer. The chemosensor had great potential applications in biological tissues.

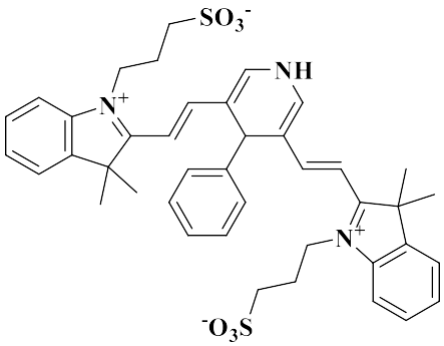

(13)

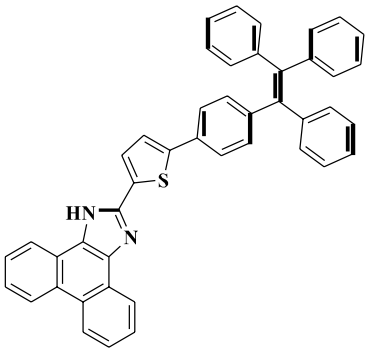

(14)

Wang et al. produced a chemosensor **14** combining the tetraphenylethylene's aggregation-induced emission (AIE) effect and phenanthro [9, 10-d] imidazole's CN^- acceptor ability to create a blue-green fluorescent CN^- chemosensor that is AIEE-active [27]. The chemosensor demonstrated both the mechanofluorochromic (MFC) phenomena and the AIEE characteristic in two different solvents (DCM/n-hexane and THF/H_2O) which allowed the highly selective and sensitive detection of CN^- ion. Due to the intramolecular charge transfer (ICT) mechanism, the chemosensor exhibited a significant Stokes shift at 107 nm. The higher Stokes shift (184 nm) was produced by the CN^- that caused the fluorescent color to change from blue-green to sodium-yellow and naked eye color change from light yellow to dark yellow. The detection limit was evaluated to be 0.09258 μM.

Sun et al. synthesized a "turn-on" fluorescent chemosensor **15** based on the intramolecular charge transfer in aqueous media for CN^- [28]. The dicyanovinyl group of chemosensor was attacked by a nucleophile to provide a colorimetric and fluorimetric response to CN^- ion with the detection limit of 1.12 μM. The absorption peak at 420 nm dropped away and the emission band focused at 496nm significantly increased after adding 9.0 equiv. of cyanide, thus creating a colorless detection system with bright green fluorescence.

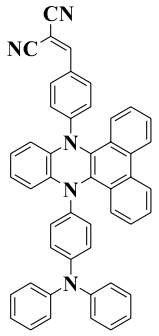

(15)

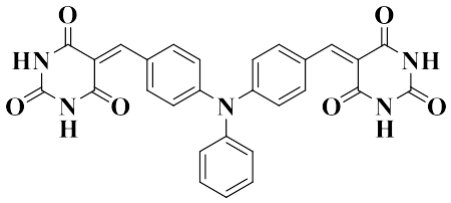

(16)

Zuo et al. designed a fluorescent chemosensor **16** having triphenylamine moiety and further investigated its sensing behavior towards various anions via AIE properties [29]. The absorption band was observed at 350 nm; however, when incubation with CN^- was done absorption band appeared at 474 nm, and the fluorescence intensity at 581 nm steadily decreased due to the interruption of ICT of chemosensor in DMSO: H_2O ratio. With the pH range of 1-9.0, the detection limit was found to be 2.95×10^{-8}mol/L with the binding ratio of 1:2 was evaluated using job's plot. The chemosensor was used to detect CN^- in industrial wastewater.

Bai et al. synthesized a reversible "turn-on" fluorescent and colorimetric chemosensor **17** for the detection of CN^- ion [30]. It was observed that chemosensor showed an absorption band at 470 nm while two emission bands at 380 and 470 nm. With the addition of CN- ion, the absorption band grew in intensity while the emission bands at 380 and 470 nm exhibited decreased and increased intensity respectively. The color of the solution changed from colourless to yellow under UV light with CN^- only. On the other hand, no interferences from other ions were detected; hence, it was highly selective towards CN^- only. According to the Benesi– Hildebrand plot, binding constant of **17** with CN^- was found to be 1.81×10^5 M^{-1} with the detection limit of $9.4\times10^-$

[10] M. The synthesized chemosensor can be used to detect CN^- in tap water, food samples, and living systems.

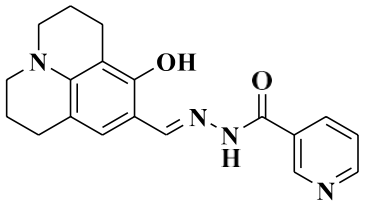

(17)

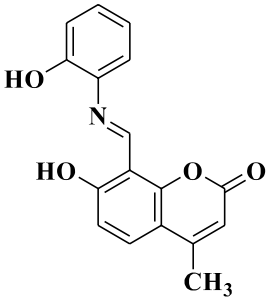

(18)

Ding et al. synthesized a chemosensor **18** which is based on coumarin derivative for the detection of CN^- [31]. **18** could serve as "turn-on" fluorescent chemosensor for the CN^- detection in DMSO: H_2O system. It was observed that the chemosensor showed a strong and weak absorption band at 350 and 456 nm due to π–π* and n–π* transition respectively. In fluorescence, the weak emission band occurred at 476 nm. The incremental addition of CN^- led to the red shift from 350 nm to 372 nm in absorption while the fluorescence intensity increases with blue shift of 29 nm. In absorption and fluorescence spectra the detection limit was found to be 5.3×10^{-7} M and 3.8×10^{-8} M respectively.

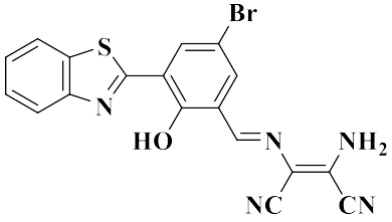

(19)

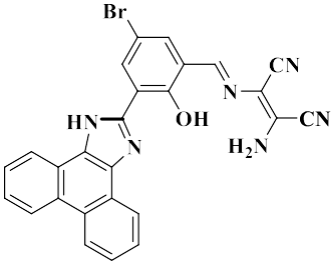

(20)

Erdemier et al. synthesized two fluorogenic and colorimetric chemosensors **19&20** based on diaminomaleonitrile moiety for the detection of CN^- ions [32]. On the addition of CN^- ion, the fluorescence intensity of chemosensor **19** was increased while the fluorescence intensity of chemosensor **20** was quenched due to the push-pull ICT system. With low detection limits of 0.92 and 0.68 μM respectively, calorimetrically both the chemosensors demonstrated different color changes for CN^- sensing in aqueous CH_3CN. The yellow-colored solutions of both **19** and

20 turned dark pink and somon pink respectively. The selective detection of CN^- can be carried out using smart-phone based technology that could read out the color value immediately.

1.3.Research Gap

Many studies in the scientific literature have unveiled the utility of Schiff base chemosensors employing benzimidazole. The benzimidazole has been proven to be useful in the area of analyte detection and sensing, owing to its inherent fluorescent properties. By altering distinct positions of the benzimidazole molecule to generate different derivatives, the photophysical characteristics of these chemosensors can be moderated. However, as per the latest reports available in the literature, the exploration and documentation of ratiometric fluorescent chemosensors based on benzimidazole that could be used for the detection of CN^- ion in aqueous solution remain relatively limited. So, the present study aimed at design and synthesis of benzimidazole appended Schiff base which on reaction with aromatic aldehydes resulted in the formation of ratiometric fluorescent chemosensor that could selectively detect CN^- ions relevant to both biology and environment.

1.4.Objectives

On the basis of studied research gap, the following objectives were designed:

- Design and Synthesis of novel Schiff bases by appending benzimidazole derivative with aromatic aldehydes.
- To demonstrate the photophysical properties of the synthesized Schiff bases towards various cations and anions.

CHAPTER 2

Experimental Section

2.1.Materials and Methodology

All the chemicals and reagents were purchased from different suppliers such as Sigma Aldrich, Loba Chemicals and Spectrochem, which were further used without any purification. For photophysical studies, HPLC grade solvents from Spectrochem were used. Thin Layer Chromatography (TLC) was the major technique that was used to monitor the progress of the reaction. The structure characterization was done by ^{1}H-NMR and ^{13}C-NMR spectra, recorded on JEOL ECX-400 MHz using the solvents $CDCl_3$ and DMSO-d_6 as the samples were soluble in these. TMS (trimethylsilane) was used as reference to record the chemical shift in ppm. The instrument named as XEVO G2-XS QTOF of Waters (USA) was used to record the mass spectra. The absorption spectra were carried out using UV–Vis Spectrophotometer (SHIMADZU-2600) and fluorescence spectra were carried out in Cary Eclipse fluorescence Spectrophotometer. The excitation and emission slit widths in fluorescence spectrophotometer were 10 and 20 respectively. The DLS was performed on Zeta potential analyzer (ZEN 3600) instrument.

2.2.Preparation of Solution

The stock solution of chemosensor **3** (10^{-3} M) was prepared using CH_3CN: DMSO [95:5(v/v), 20 μM)] and all the anions (10^{-1}M) were prepared in CH_3CN at different concentrations. For UV-vis and fluorescence investigations, the stock solution of 10^{-3} M chemosensor **3** was diluted to 20 μM using CH_3CN. The different anions such as CN^-, SCN^-, Cl^-, F^-, DCP, $P_2O_7^{4-}$, NO_3^-, Br^-, I^-, HSO_4^-, $H_2PO_4^-$, and CH_3COO^- were added as their tetrabutyl ammonium salts. The solutions were allowed to settle after each addition before being scanned.

2.3.Binding Constant

The strength of the interaction between the chemosensor **3** and different analytes can be determined by using a mathematical equation called the Benesi-Hildebrand equation.

$$\frac{1}{I - I_o} = \frac{1}{K_a\,(I_{m\,a}\chi - I_o)[C]^n} + \frac{1}{I_{m\,a}\chi - I_o}$$

Where,

C = concentration of analyte

K_a =binding constant to be determined

n = number of analytes bound to a single molecule of ligand

I = the absorption and emission intensity in absence of analyte

I_o = the absorption and emission intensity at an intermediate concentration

I_{max} = refers to the concentration at which the analyte interacts with the ligand completely

Detection limit (DL) can be evaluated by equation mentioned below:

$$DL = \frac{2 \times \text{Standard deviation of the blank solution}}{\text{slope of calibration curve}}$$

2.4.Job's Plot

The different solutions of varying concentrations of chemosensor **3** and CN^- were prepared. The total volume of both the chemosensor **3** and CN^- was kept the same, thus changing the concentration of either the CN^- or the chemosensor **3** during each measurement. The measured intensity was then plotted against the mole fraction of CN^- ions at specific wavelength.

2.5. pH titrations of chemosensor 3

For varying the pH of the solution 0.1 M solutions of HCl and NaOH were prepared in double distilled water and the pH was recorded on Sistronics pH-meter, having Pt-electrode. The pH titrations were performed using H_2O. After every addition of 0.1 M NaOH/HCl the solutions were properly stirred for maintaining the homogeneity of the solution and were kept undisturbed for minimum 2 min. After maintaining the pH, the absorption and emission spectra were recorded and plot between varying pH and intensity at λ_{abs} = 355 nm and λ_{em} = 450 nm and 530 nm for chemosensor **3** was made.

2.6.Experimental Section

2.6.1.Synthesis of Compound 1 (2-(5-nitro-1H-benzo[d]imidazol-2-yl) phenol):

p-nitrophenylene diamine (0.5g, 3.26 mmol) was added to the solution of salicylaldehyde (0.47g, 3.84 mmol) and were mixed in nitrobenzene. The reaction was refluxed for 12 hours till the reaction completion was indicated using TLC in ethyl acetate: hexane (2:8, v/v) as solvent system. A brown colored compound **1** was obtained. The product was filtered and washed with

diethyl ether and hexane. 94% Yield [33]

2.6.2.Synthesis of Compound 2 (2-(5-amino-1H-benzo[d]imidazol-2-yl) phenol):

Compound **1** (0.50g, 1.95 mmol) and sodium dithionite (2.389g, 11.6 mmol) were added to the solution of 30 ml THF, 10 ml H_2O and 15 ml NH_3. The reaction was stirred for 30 minutes at room temperature. The progress of the reaction was monitored using TLC in ethyl acetate: hexane (2:8, v/v) as solvent system. The separation was done using ethyl acetate and water which was filtered and dried. A brown colored solid compound **2** was obtained. 47% Yield [33]

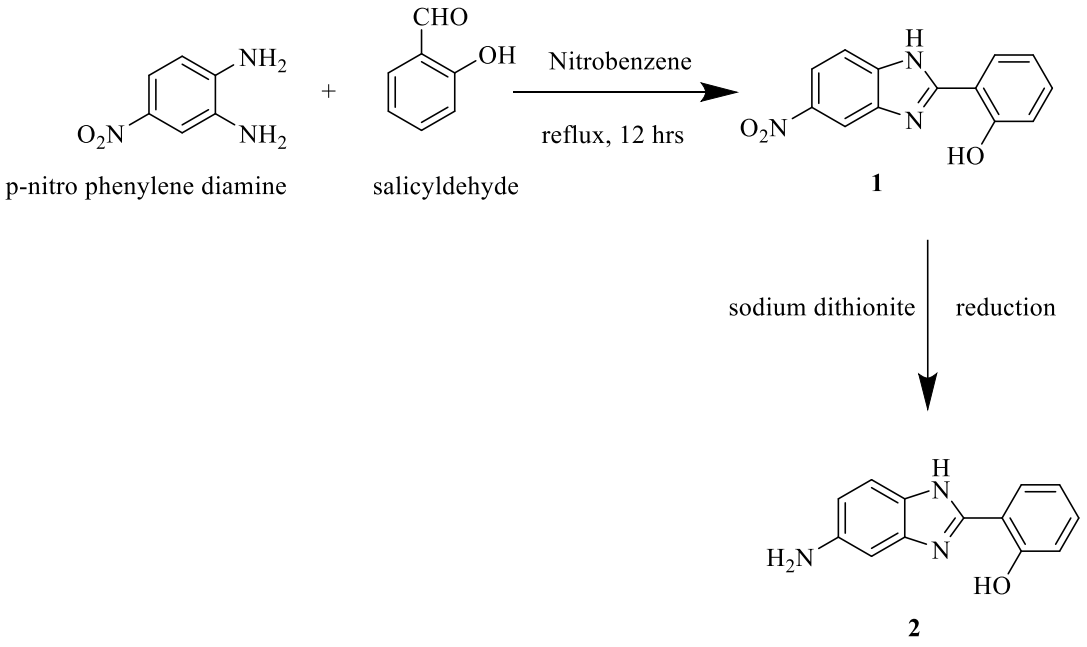

Scheme 1: Synthesis of compound 1 and 2

2.6.3.Synthesis of Chemosensor 3 [(E)-1-(((2-(2-hydroxyphenyl)-1H-benzo[d]imidazol-5-yl) imino) methyl) naphthalen-2-ol]:

Compound **2** (0.20g, 0.88 mmol) and 2-hydroxy-1-napthaldehyde (0.168g, 0.97 mmol) were mixed in ethanol. The reaction was refluxed for 12 hours and monitored continuously via TLC. As the reaction completion was indicated, a brown colored solid (chemosensor **3)** was obtained that was filtered, washed and dried. Further, chemosensor **3** was recrystallized using ethanol which was again filtered and dried to obtain the pure brown colored chemosensor **3**. 61% Yield, M.pt 265-267 ^oC, ^1H NMR (DMSO-d_6, 400 MHz); δ 9.73 (s, 1H), 8.53 (d, J = 8 Hz, 1H, Ar-H), 8.06 (d, J = 8 Hz, 1H, Ar-H), 7.90 (d, J = 12 Hz, 1H, Ar-H), 7.77 (d, J = 8 Hz, 2H, Ar-H),

7.52 (t, *J* = 16 Hz, 2H, Ar-H), 7.37–7.32 (m, 2H, Ar-H), 7.04–6.99 (m, 3H, Ar-H); ^{13} C NMR (DMSO-d_6, 100 MHz): δ 158.48, 153.36, 136.93, 133.65, 132.48,129.50, 128.54, 127.18, 126.93, 123.90, 122.52, 120.95, 119.77, 117.76, 113.09, 109.17; HRMS(ESI-MS): (m/z) $[M+H]^+$ calcd for $C_{24}H_{17}N_3O_2$: 380.1321, found: 380.0142.

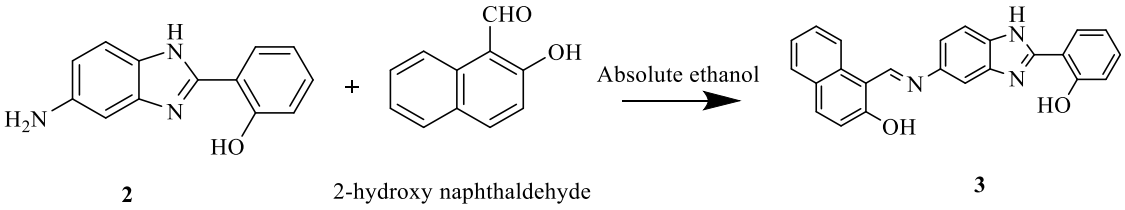

Scheme 2: Synthesis of chemosensor 3

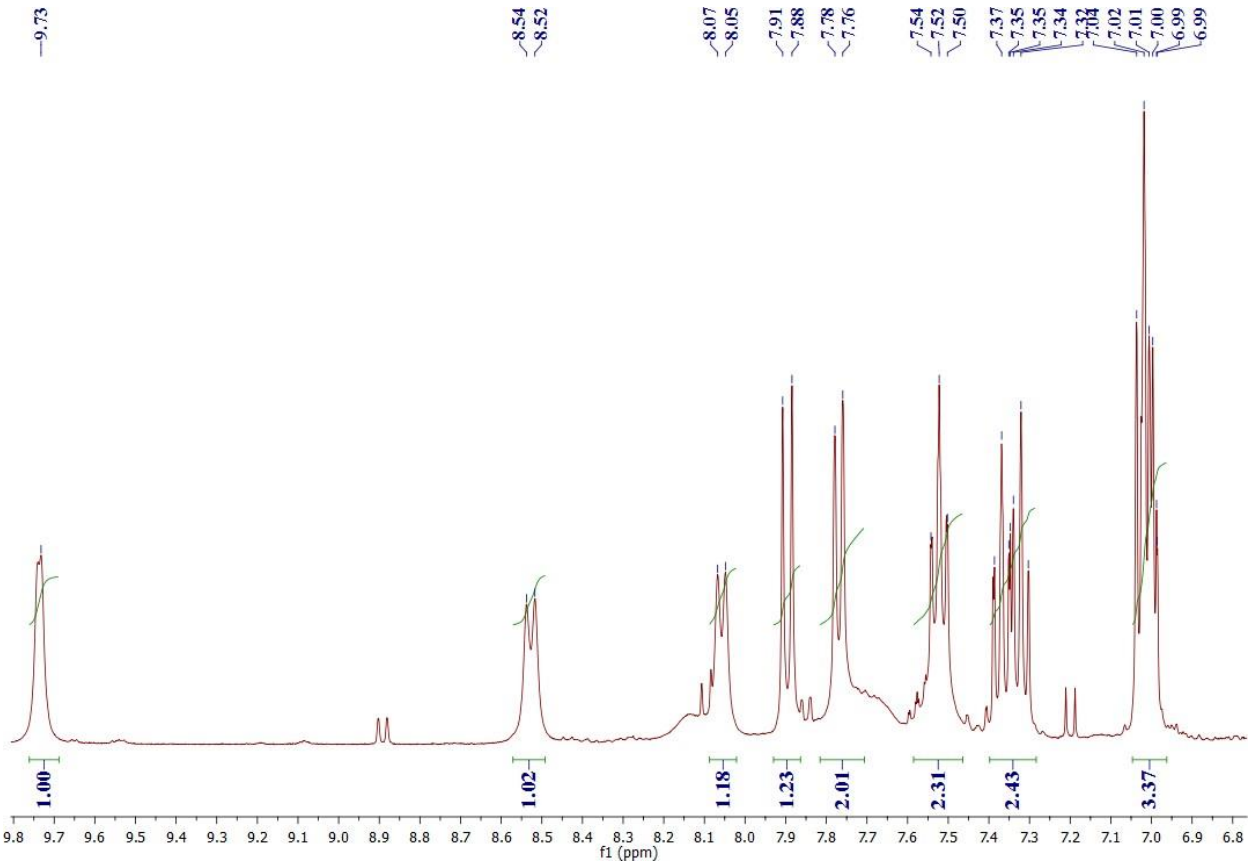

Figure 1: ^{1}H NMR of Chemosensor 3

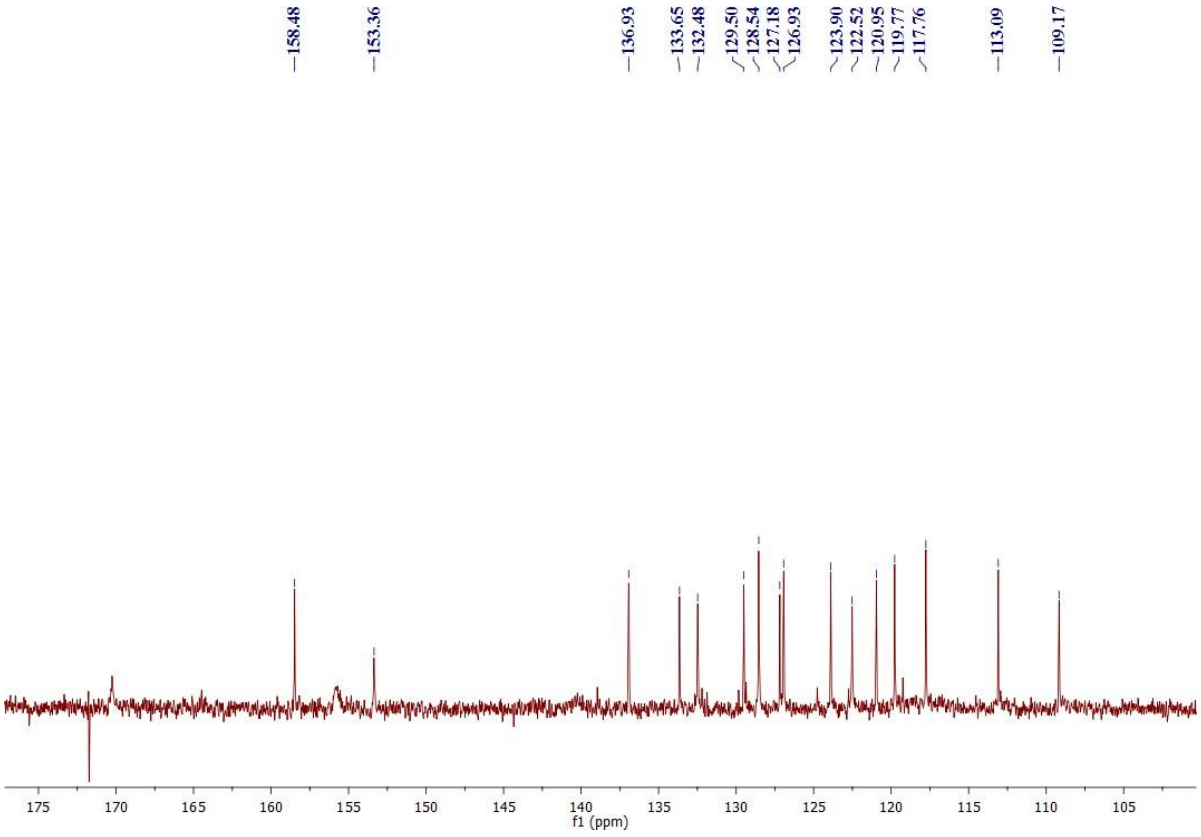

Figure 2: ^{13}C NMR of Chemosensor 3

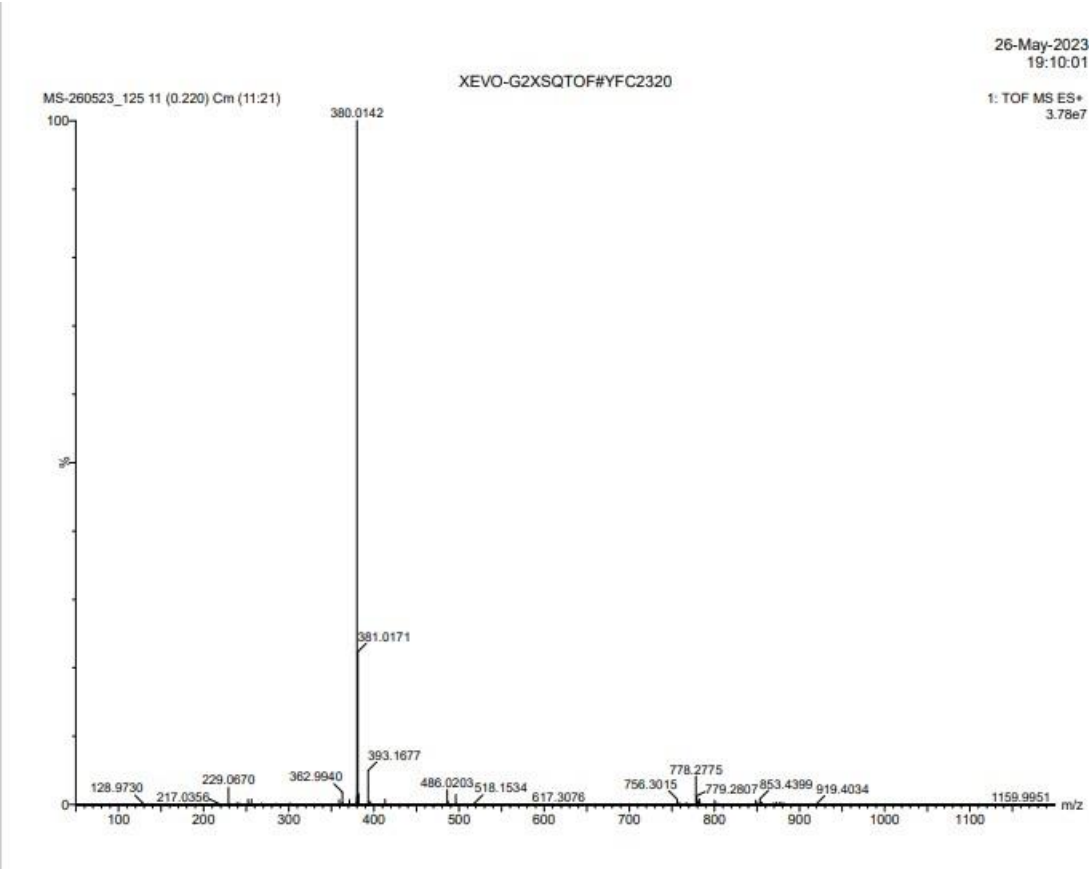

Figure 3: HRMS of Chemosensor 3

CHAPTER 3

RESULTS AND DISCUSSION

3.1.Evaluation of photophysical properties of chemosensor 3

The photophysical characteristics of chemosensor **3** were investigated using absorption and emission spectroscopy. The absorption peak of chemosensor **3** (20 µM, CH_3CN) was observed at 385 nm and upon excitation at this wavelength, the emission peak was observed at 475 nm accompanied with stokes shift of 90 nm. The visible color changes from colorless to dark yellow and blue to yellow in fluorescence was seen **(Figure 4a-4b)**. To observe the effect of solvent polarity on the photophysical properties of chemosensor **3**, absorption and emission spectra were recorded in different solvents of varying polarity. On increasing the polarity of the system (from non-polar cyclohexane, hexane, dioxane, THF to polar H_2O) chemosensor **3** displayed a red shift with the formation of two new bands, one at 470 nm while other at 530 nm in absorption spectra while at 450 nm and 560 nm in the emission spectra, thus demonstrating the presence of ICT phenomenon **(Figure 4c-4d)**. The presence of both a basic C=N- (imine unit) and an acidic -OH group (phenolic unit) in chemosensor **3** enabled proton transfer through keto-enol tautomerism. However, in polar environments, the emission moves towards the low stokes shift of 65 nm at 450 nm and high stokes shift of 175 nm at 560 nm. This suggests that the low stokes shift emission at 450 nm in a highly polar environment can be due to the enol form, while the emission with high Stokes shift can be due to the tautomeric keto form.

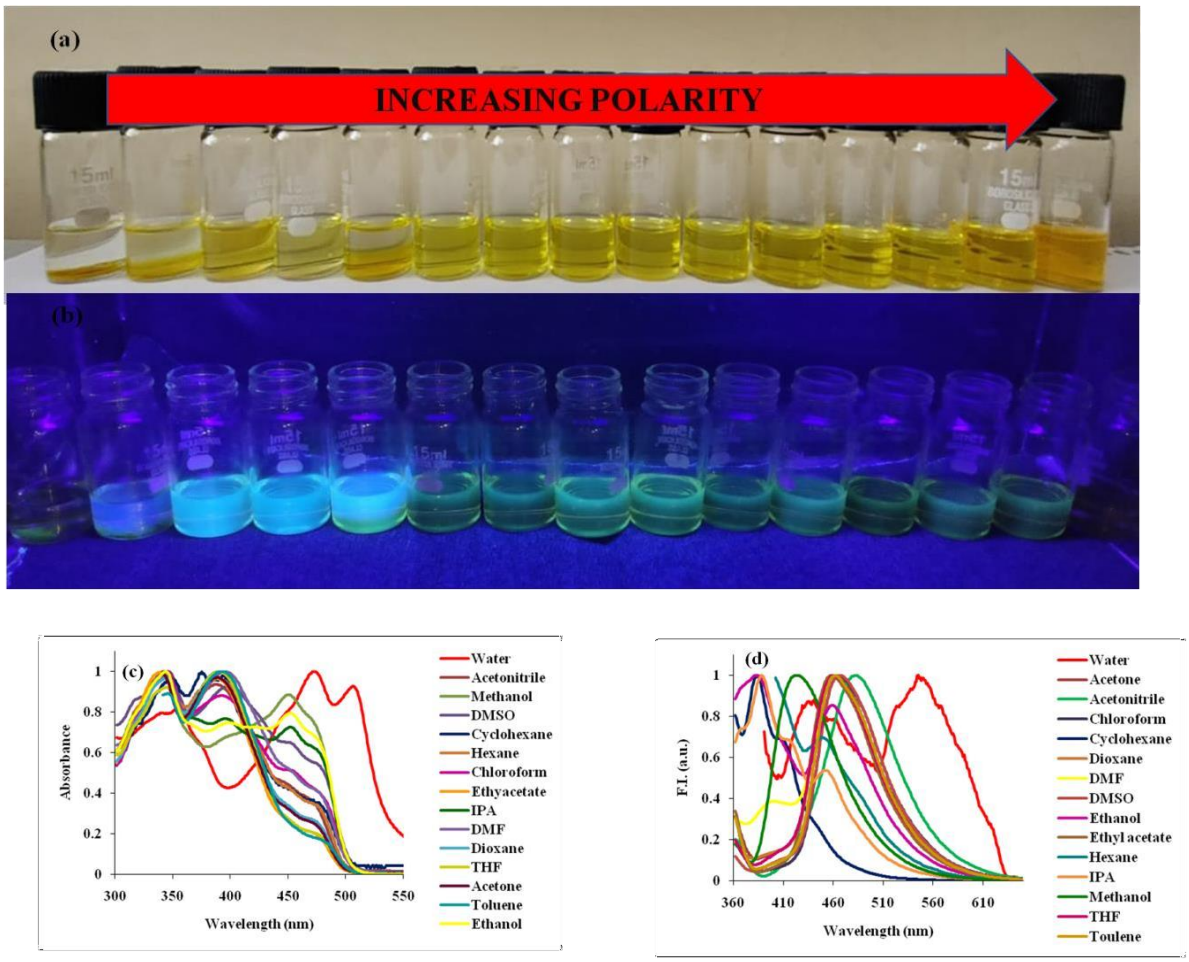

Figure 4: (a) Visual color changes of chemosensor 3 (20 µM) in different solvents (b) Effect of different solvents on solution of chemosensor 3 (20 µM) under UV light (c) Absorption and (d) emission spectra of chemosensor 3 in different solvents.

Table 1: Photophysical properties of chemosensor 3

S.No.	Solvent	λ_{max} (nm)	Molar absorptivity Constant $\varepsilon=M^{-1}\,cm^{-1}$	λ_{em} (nm)	Stokes Shift $\Delta\nu$ (cm^{-1})
1	Hexane	385	49500	475	4921
2	Cyclohexane	350	47000	450	6349
3	Toulene	385	46000	475	4921
4	Chloroform	385	43500	475	4921
5	THF	385	47500	475	4921
6	Dioxane	385	48000	475	4921
7	Ethyl Acetate	385	48500	475	4921
8	DMSO	385	45500	475	4921
9	Acetonitrile	385	48500	490	4921
10	IPA	350	46000	450	6349
11	Ethanol	350	47000	475	7518
12	Methanol	350	43000	430	5315
13	DMF	385	49000	475	4921

14	Acetone	385	49000	475	4921
15	Water	470	46500	560	3419

3.2.Aggregation induced emission (AIE) characteristics of chemosensor 3:

The absorption and emission spectra of chemosensor **3** were investigated to analyse its AIE (Aggregation-Induced Emission) characteristics. The AIE property of chemosensor **3** was investigated in the good solvent (CH_3CN) with the gradual addition of poor solvent (H_2O) using the absorption and emission spectra. The solution of chemosensor **3** (20 μM, CH_3CN) displayed an absorption maxima at 385 nm. The fluorescence images of chemosensor **3** in H_2O: CH_3CN ratio resulted in strong yellow emission in visual and long UV light **(Figure 5a-5b).** The absorption intensity of chemosensor **3** decreased at 385 nm upto 20% H_2O addition. However, a shift in band was observed from 385 nm to 455 nm with associated decrease in intensity as the H_2O ratio was increased from 30% to 50%. With progressive increase of H_2O ratio to chemosensor **3** (from 60-90% H_2O:CH_3CN; v/v), two new bands appeared at 450 nm and 530 nm along with the decrease in absorption intensity. With increasing the H_2O content in CH_3CN, the absorption maxima experienced a red shift, leading to the formation of J-type aggregates **(Figure 5c)**. In the emission spectra, the emission intensity of chemosensor **3** at 475 nm decreased up to 60% H_2O: CH_3CN. However, on raising the H_2O content to 70–90% the blue shift was caused with the formation of two bands at 450 nm and 530 nm.The emisssion intensity of chemosensor **3** at 450 nm was decreased while at 530 nm it increased from 70% to 90% H_2O: CH_3CN ratio **(Figure 5d)**. The increase in intensity at ESIPT band indicated the protection of H-Bonding in the form of aggregates. Hence, the emission at 530 nm in aggregated form would be due to restriction in intramolecular rotation around C-N, N- N, and C=N bonds and allowing proton transfer.

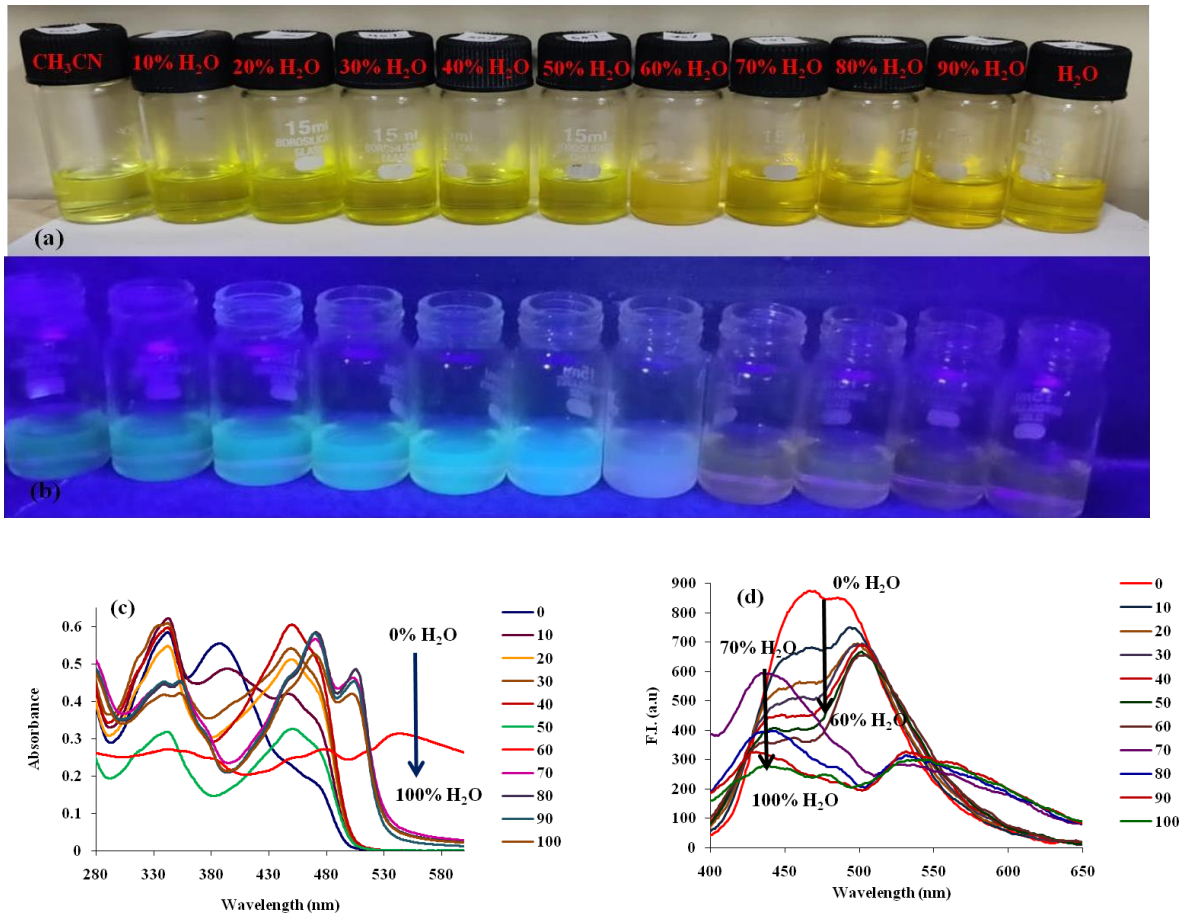

Figure 5: (a) Visual color change of chemosensor 3 in different H_2O: CH_3CN ratio (b) Change in UV light of chemosensor 3 in H_2O: CH_3CN (c) Absorption and (d) Emision spectra of chemosensor 3 (20 µM) upon increasing the volume of H_2O in CH_3CN

DLS measurements were also performed to support the aggregation behavior and to determine the size of aggregates of chemosensor **3** in the presence of various H_2O: CH_3CN volume ratios. The size of chemosensor **3** (20 µM) in pure CH_3CN was found out to be 200-900 nm approximately with the average size of 500 nm **(Figure 6a)** whereas the particle size of chemosensor **3** in 70% H_2O: CH_3CN was found to be between 350-800 nm with the average size of 600 nm **(Figure 6b)**. In pure H_2O the particle size was found to be 400-1600 nm with the average size of 900 nm for chemosensor **3 (Figure 6c)**. Hence, the particle size increased in proportion to the increased H_2O content due to the formation of aggregates.

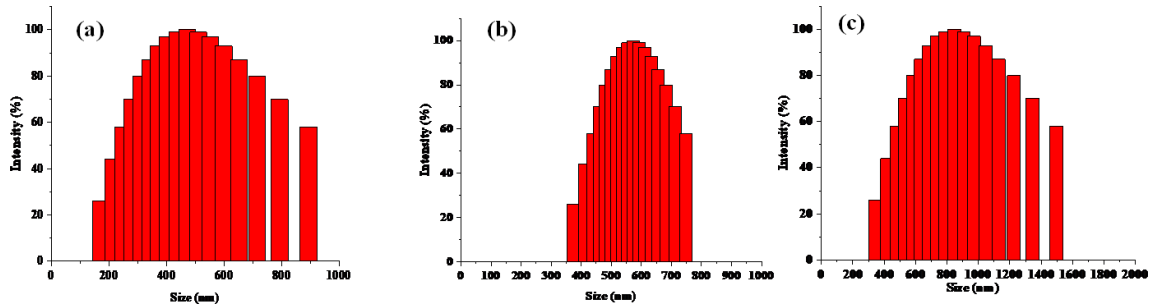

Figure 6: DLS of chemosensor 3 (20 µM) in (a) pure CH_3CN (b) H_2O: CH_3CN (70:30(v/v)) and (c) pure H_2O

3.3.Sensing properties of chemosensor 3:

The photophysical behavior of chemosensor **3** (20 µM; (CH_3OH/H_2O) (1:1); v/v) was evaluated towards several anions, including CN^-, SCN^-, Cl^-, F^-, Br^-, I^-, HSO_4^-, $H_2PO_4^-$, $P_2O_7^{4-}$, DCP and CH_3COO^- using absorption and emission spectroscopy. The chemosensor **3** displayed absorption peak at 355 nm. Upon addition of different anions to the solution of chemosensor **3**, no significant change in the absorption spectra was observed **(Figure 7a)**. Similarly, the emission properties of chemosensor **3** were also measured towards different anions. When excited at 355 nm, the emission peak was observed at 450 nm and 530 nm (20 µM, H_2O) accompanied with the visible yellow color **(Figure 7b)**. Amongst the various anions tested in aqueous medium, chemosensor **3** (20 µM) showed fluorescence enhancement **(Figure 7c)** along with blue shift only with CN^- ion. The extensive π-conjugation system created in chemosensor **3** on interaction with the CN^- ion may be the cause of the enhanced fluorescence **(Figure 7d)**. The titration experiment was performed to look into the steady state variation of chemosensor **3** upon addition of CN^- ions. After the addition of 360 µM of CN^- ion, a plateau in the fluorescence spectra was

seen. As the change in emission intensity was quite noticeable, it is reasonable to believe that the fluorescence for free chemosensor **3** was initially in the "turn off" condition and that it was later "turn on" with the addition of CN^- ion **(Figure 7e)**. To determine the selectivity of chemosensor **3** towards CN^-, emission spectra of the complex was taken in the presence of other competitive anions. The findings of interference study led to the conclusion that no other anion interfered in the chemosensor **3**-CN^- complex, indicating that chemosensor **3** exhibits selectivity for CN^- ion even when other anions are present **(Figure 8)**.

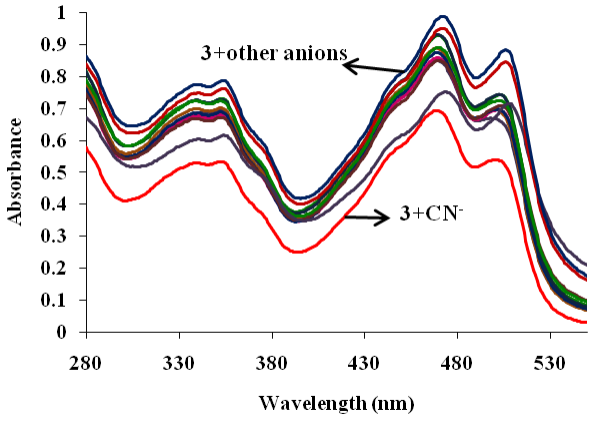

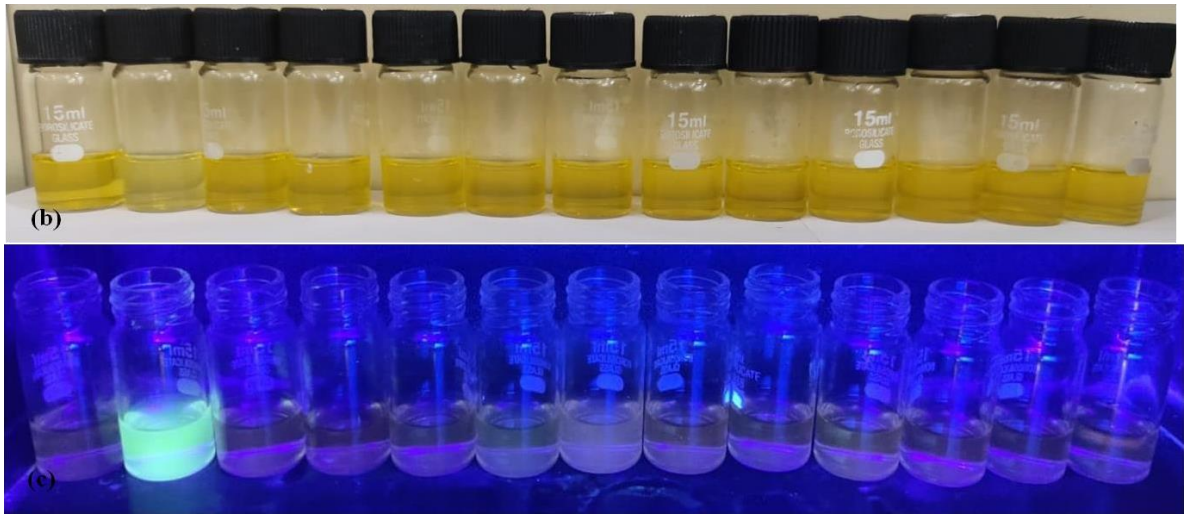

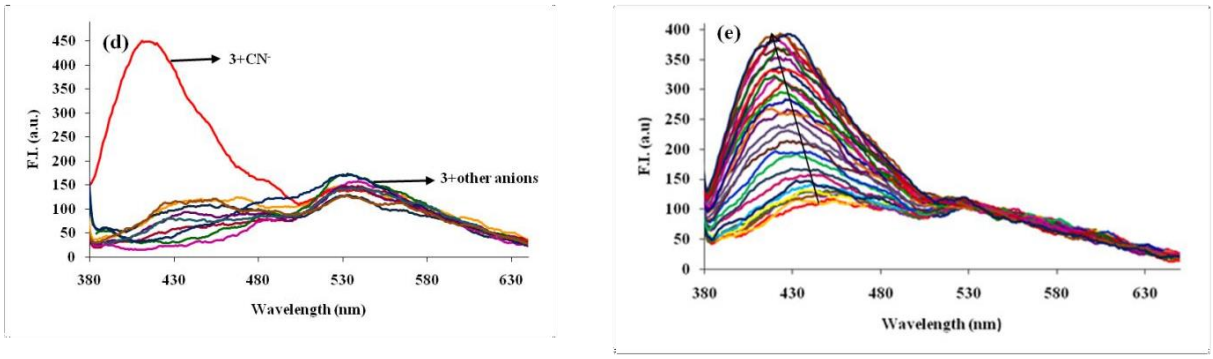

Figure 7: **(a) Absorption spectra of chemosensor 3 (20 µM; H2O) in the presence of different anions (1000 µM) (b) Visual color change of different anions on solution of chemosensor 3 (20 µM; H2O) (c) Effect of different anions on solution of chemosensor 3 (20 µM; H2O) under UV light (d) Emission spectra of chemosensor 3 (20 µM; H2O) in the presence of different anions (1000 µM) and (e) Emission spectra of chemosensor 3 (20 µM; H2O) with incremental addition of 0-360 µM CN^- ions.**

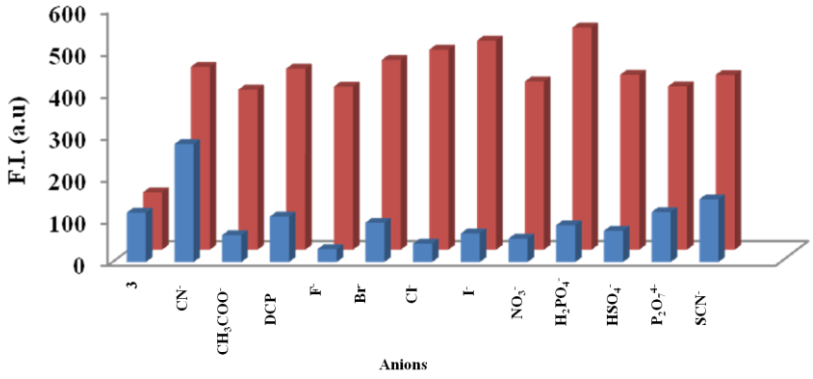

Figure 8: Relative intensity of chemosensor 3 (20 µM) in H2O (λex= 355 nm) with different competing anionsin the presence & absence of CN^- ion (λem= 450nm), where blue bar represent the variation in emission intensity of chemosensor 3 with different anions and red bars represent various competing anions added to chemosensor 3.CN^-.

3.4.Stoichiometry, binding constant and detection limit:

Using a job's plot, the stoichiometry of chemosensor **3** and CN^- was examined. In the experiment, the spectrum response of CN^- ions at various mole fractions was measured. A maximum at 0.4 mole percent of CN^- ions was seen in the graph of fluorescence intensity against mole fraction of CN^- ions, indicating a 1:1 (chemosensor **3**:CN^-) stoichiometry **(Figure 9a)**. Additionally, a good linear relationship was used to calculate the binding constant for chemosensor **3**.CN^-, using the Benesi-Hildebrand equation which was observed to be 2×10^{-3} M^{-1}

(Figure 9b). The limit of detection for chemosensor **3** towards CN^- ions was calculated to be 3.3×10^{-7} M using the standardized IUPAC equation **(Figure 9c)**.

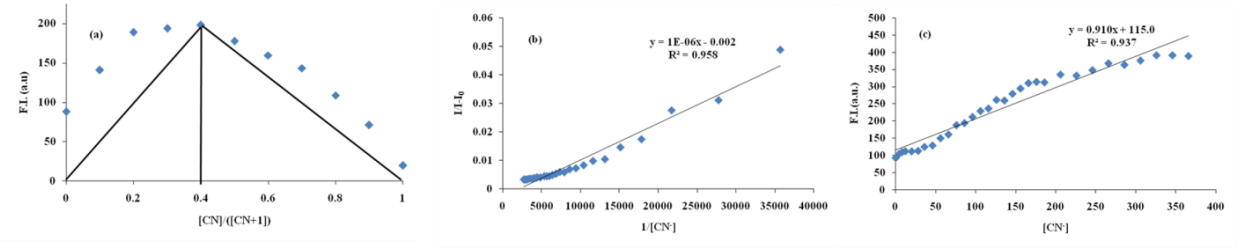

Figure 9: (a) Job's plot of chemosensor 3 in H_2O (b) Binding constant for chemosensor 3. (c) Detection limit of CN^- ions

3.5.Effect of pH on chemosensor 3

The pH stability of chemosensor **3** was also evaluated at emission intensity values of 450 nm and at 530 nm. An acid-base titration was performed which revealed that chemosensor **3** was stable in the pH range of 3-11 establishing its benefit for rapid monitoring in environmental and biological backgrounds. The presence of imine (-C=N-) and hydroxyl group (-OH) can lead to the protonation or deprotonation of chemosensor **3** depending on whether the medium is acidic or basic. At 450 nm, the fluorescence intensity of chemosensor **3** increased in the basic medium (pH 8-11) whereas negligible change was observed in the acidic medium. Likewise, chemosensor **3** was stable in the pH range of 6-11 at 530 nm. Below pH 6 (acidic medium) there was increase in the intensity at 530 nm **(Figure 10)** which might have been caused by the deprotonation of hydroxyl oxygen atom and imine nitrogen atom thus preventing the ESIPT process [34]

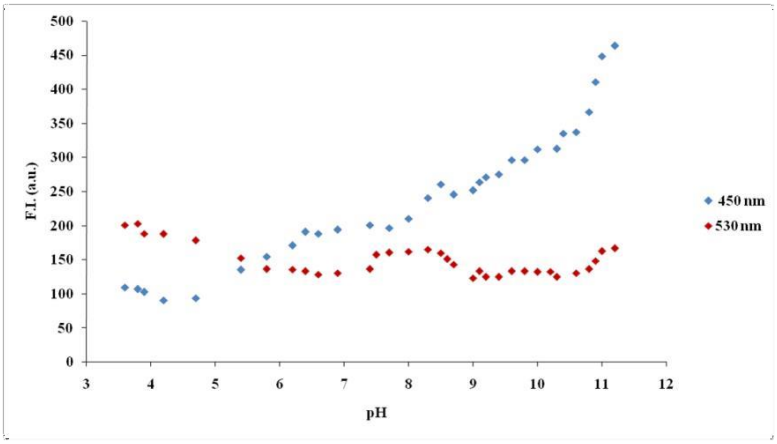

Figure 10: Effect of pH on chemosensor 3 at 450 nm and 530 nm

3.6.Time-correlated single photon counting (TCSPC) study: -

The enhancement in the fluorescence intensity on binding with the CN^- ion has been supported by the results obtained from fluorescence decay measurements, using the TCSPC study. The fluorescence decay behavior of chemosensor **3** and its complexes are best fitted in third exponential function at 450 nm. At 450 nm, chemosensor **3** showed three components with lifetime values of 0.21 ns, 3.03 ns and 10.62 ns having the population of 0.01, 0.76 and 0.21 % respectively. The average life time for chemosensor **3** was evaluated to be 2.8 ns. Upon the addition of CN^- to the solution of chemosensor **3**, again three components were obtained with life time of 3.10 ns, 0.17 ns and 4.92 ns at 450 nm. The population of all the components was 0.80, 0.01 and 0.17% respectively **(Table 1)**. The average life time was calculated to be 2.51ns. The average life time was decreased from 2.8 ns to 2.51 ns which indicated that the chemosensor **3** bind with CN^- ion in dynamic manner.

Table1: - Fluorescence lifetime measurements for chemosensor 3 and its complex with CN^- ion in H_2O

H_2O	Wavelength (nm)	τ_1 (ns)	τ_2 (ns)	τ_3 (ns)	α_1	α_2	α_3	χ^2	τ_{av} (ns)
Chemosensor 3	450 nm	0.21	3.03	10.62	0.01	0.76	0.21	1.05	2.8
Chemosensor 3 + CN^-	450 nm	3.10	0.17	4.92	0.80	0.01	0.17	1.02	2.51

Conclusions

In summary, we have successfully synthesized a novel Schiff base chemosensor **3,** appended with benzimidazole incorporating 2-Hydroxy-1-napthaldehyde. Chemosensor **3** showed excellent photophysical properties demonstrating intramolecular charge transfer phenomenon in aqueous medium and aggregation-induced emission in >70% H_2O-CH_3CN system. Chemosensor **3** exhibited fluorescence "Turn-On" behavior in aqueous medium on interaction with CN^- ion. In fluorescence spectra, chemosensor **3** displayed two bands, one at 450 nm and other at 530 nm. Upon addition of CN^- ion to chemosensor **3**, the emission spectra blue shifted to 410 nm followed by a fluorescence color change from yellow to blue. Moreover, the extensive π-conjugation system was developed in chemosensor **3**, which led to the fluorescence enhancement with the CN^- ion. Chemosensor **3** displayed selectivity towards CN^- ions with limit of detection of 3.3×10^{-7} M and binding constant value of 2×10^3 M^{-1}. The binding ratio of chemosensor **3** with CN^- was evaluated to be 1:1 via Job's plot.

Future Scope

As chemosensor **3** exhibited selectivity towards the CN^- ion, so the scope of detection can be extended to the numerous applications of CN^- ion sensing in many sectors, including cell bioimaging, organic lighting emitting diode (OLED) devices, molecular keypad lock and real water sample analysis.

References

[1] S. Anbu, A. Paul, K. Surendranath, N.S. Solaiman, A.J.L. Pombeiro, A benzimidazole-based new fluorogenic differential/sequential chemosensor for Cu^{2+}, Zn^{2+}, CN^{-}, $P_2O_7^{4-}$, DNA, its live-cell imaging and pyrosequencing applications, Sensors and Actuators: B. Chemical 337 (2021) 129785.

[2] A. Tigreros, J. Portilla, Recent progress in chemosensors based on pyrazole derivatives, RSC Advances, 10 (2020) 19693–19712.

[3] X.-L. Hu, H.-Q. Gan, F.-D. Meng, H.-H. Han, D.-T. Shi, S. Zhang, L. Zou, X.-P. He, T.D. James, Fluorescent probes and functional materials for biomedical applications, Frontiers of Chemical Science and Engineering, (2022) 1-13.

[4] X. Chen, Z. Chen, Y. Hu, L. Ma, Z. Zhang, F. Yi, H. Zhang, C. Liu, Novel quinolinium-derivated fluorescent fluoride chemosensor based on the F^{-} triggred cascade reaction, Tetrahedron Letters, 100 (2022) 153870.

[5] A.L. Berhanu, I. Mohiuddin, A.K. Malik, J.S. Aulakh, V. Kumar, K.-H. Kim, A review of the applications of Schiff bases as optical chemical sensors, TrAC Trends in Analytical Chemistry, 116 (2019) 74-91.

[6] N. Kumari, S. Singh, M. Baral, B.K. Kanungo, Schiff Bases: A Versatile Fluorescence Probe in Sensing Cations, Journal of Fluorescence, 33 (2023) 859–893.

[7] D. Udhayakumari, V. Inbaraj, A Review on Schiff Base Fluorescent Chemosensors for Cell Imaging Applications, Journal of Fluorescence, 30 (2020) 1203-1223.

[8] P. Ravichandiran, A.B. Czubara, M. Maslyk, A.P. Bella, P.M. Johnson, S.A. Subramaniyan, K.S. Shim, D.J. Yoo, A phenoxazine-based fluorescent chemosensor for dual channel detection of Cd^{2+} and CN^{-} ions and its application to bio-imaging in live cells and zebrafish, Dyes and Pigments, 172 (2020) 107828.

[9] X. Jia, Y. Yang, H. Zhai, Y. Liu, Y. He, Q. Ma, Y. Liu, Theoretical insights into the spectral properties of a salicylideneanilinebased fluorescence chemosensor (SB1) and its sensing mechanism for cyanide anion, Journal of Molecular Liquids 312 (2020) 113295.

[10] A.I. Said, D. Staneva, S. Angelova, I. Grabchev, A multi-channel rhodamine-pyrazole based chemosensor for sensing pH, Cu^{2+}, CN^{-} and Ba^{2+} and its function as a digital comparator, Journal of Photochemistry & Photobiology, A: Chemistry 433 (2022) 114218.

[11] H.-H. Yang, P.-P. Liu, J.-P. Hu, H. Fang, Q. Lin, Y. Hong, Y.-M. Zhang, W.-J. Qu, T.-B. Wei, A fluorescent supramolecular gel and its application in the ultrasensitive detection of CN^{-} by anion–π interactions, The Royal Society of Chemistry 16 (2020) 9876-9881.

[12] D. Yang, X. Diao, J. Liu, Y. Leng, X. Cai, A Novel and Reactive Fluorescent "Turn-on" Probe Based on Benzimidazole Derivative for Selective CN^{-} Detection, Journal of Inorganic and General Chemistry 648 (2022) 202100311.

[13] G. Jindal, P. Vashisht, N. Kaur, Benzimidazole appended optical sensors for ionic species: Compilation of literature reports from 2017 to 2022, Results in Chemistry 4 (2022) 100551.

[14] E. Kandemir, M. Özkütük, B. Aydıner, N. Seferoglu, H. Erer, Z. Seferoglu, Novel fluorescent coumarin-thiazole based sensors for selective determination of cyanide in aqueous media, Journal of Molecular Structure 1249 (2022) 131593.

[15] R. Mehta, K. Paul, V. Luxami, 1-Oxo-1H-phenalene-2,3-dicarbonitrile Based Sensor for Selective Detection of Cyanide ions in Industrial Waste, Journal of Molecular Structure 1234 (2021) 130077.

[16] S.M. Kumar, D. Jothi, S.K. Munusamy, S. Enbanathan, S.K. Iyer, Imidazole-derived new colorimetric/fluorometric chemosensor for the sensitive recognition of CN^- ions: Real-time application in food samples and fluorescence bio-imaging, Journal of Photochemistry & Photobiology, A: Chemistry 434 (2023) 114269.

[17] S. Ghosh, S. Paul, S. Halder, M. Shit, A. Karmakar, J.B. Nandi, K. Jana, C. Sinha, Trace level CN^- measurement by 'turn-on' emission using Coumarinyl-Benzothiazolyl Schiff base probe in living and non-living environment, Journal of the Indian Chemical Society 100 (2023) 100957.

[18] Y. Yao, X.-M. Fu, J.-H. Hu, Novel high sensitivity dual-channel chemosensor for detecting CN^- based on asymmetric azine derivatives in aqueous media, Inorganic Chemistry Communications 141 (2022) 109557.

[19] H.-X. Liu, X.-M. Fu, J.-H. Hu, AIE based colorimetric and fluorescent sensor for the selective detection of CN^- in aqueous media, Inorganic Chemistry Communications 142 (2022) 109662.

[20] Y.-F. Song, W.-N. Wu, X.-L. Zhao, Y. Wang, Y.-C. Fan, X.-Y. Dong, Z.-H. Xu, A simple colorimetric and fluorometric probe for rapid detection of CN^- with large emission shift, Spectrochimica Acta Part A: Molecular and Biomolecular Spectroscopy 280 (2022) 121540.

[21] D. Jothi, S.K. Munusamy, S.M. Kumar, S. Enbanathan, S.K. Iyer, A benzothiazole-based new fluorogenic chemosensor for the detection of CN^- and its realtime application in environmental water samples and living cells, RSC Advances, 12 (2022) 8570–8577.

[22] V. Hemalatha, V.V. Kumar, A highly selective colorimetric sensing of CN^- ion by a hydrazine appended Schiff base and its application in detection of CN^- ion present in tobacco and food samples, Inorganic Chemistry Communications 144 (2022) 109894.

[23] N. Maurya, A.K. Singh, A chromogenic and fluorogenic chemodosimeter for selective detection of CN^-, Inorganica Chimica Acta 499 (2020) 119156.

[24] A. Ozdemir, S. Erdemir, Phenanthroimidazole and dicyanovinyl-substituted triphenylamine for the selective detection of CN^-: DFT calculations and practically applications, Journal of Photochemistry & Photobiology A: Chemistry 390 (2020) 112328.

[25] S. Dey, C. Sen, C. Sinha, Chromogenic hydrazide Schiff base reagent: Spectrophotometric determination of CN^- ion, Spectrochimica Acta Part A: Molecular and Biomolecular Spectroscopy 225 (2020) 117471.

[26] L. Xue, R. Wang, S. Qi, H. Xu, X. Wang, L. Wu, Q. Yang, J. Du, Y. Li, A novel 100% aqueous solution near-infrared ratiometric fluorescent CN^- probe based on 1,4-dihydropyridines, with a large fluorescent emission peak shift, Talanta 225 (2021) 122100.

[27] Y. Wang, H. Liu, Z. Chen, S. Pu, Aggregation-induced emission enhancement (AIEE)-active tetraphenylethene (TPE)-based chemosensor for CN^-, Spectrochimica Acta Part A: Molecular and Biomolecular Spectroscopy 245 (2021) 118928.

[28] G. Sun, W. Chen, Y. Liu, X. Jin, Z. Zhang, J. Su, A novel colorimetric and fluorometric probe for the detection of CN^-, Dyes and Pigments 176 (2020) 108224.

[29] B. Zuo, L. Liu, X. Feng, D. Li, W. Li, M. Huang, Q. Deng, A novel fluorescent sensor based on triphenylamine with AIE properties for the highly sensitive detection of CN^-, Dyes and Pigments 193 (2021) 109534.

[30] C.-B. Bai, J. Zhang, R. Qiao, Q.-Y Zhang, M.-Y. Mei, M.-Y. Chen, B. Wai, C. Wang, C.-Q. Qu, Reversible and Selective Turn-on Fluorescent and Naked-Eye Colorimetric Sensor to Detect Cyanide in Tap Water, Food Samples, and Living Systems, Industrial and Engineering Chemistry Research 59 (2020) 8125-8135.

[31] W.-M. Ding, Y. Wu, S.-Z. Zhang, J. Li, L. Xu, Y.-X. Sun, A dual-channel 'turn-on' fluorescent chemosensor for high selectivity and sensitivity detection of CN^- based on a coumarin-Schiff base derivative in an aqueous system, Luminescence (2021) 1-11.

[32] S. Erdemir, S. Malkondu, On-site and low-cost detection of cyanide by simple colorimetric and fluorogenic sensors: Smartphone and test strip applications, Talanta 207 (2020) 120278.

[33] J. Wang, H. Li, H. Qin, Z. Su, G. Liu, S. Hou, A water-soluble benzimidazole derivative for rapidly detecting Cu^{2+} in aqueous solution, Journal of Molecular Structure 1274 (2023) 134416.

[34] A. Palta, G. Kumar, V. Luxami, Excited state double proton transfer efficient probe: Theoretical investigation and sensing ability towards Pb^{2+} and Al^{3+} ions, Journal of Photochemistry & Photobiology A: Chemistry 433 (2022) 114198.

Document Information

Analyzed document	MSc Thesis Anju Garg.doc (D172403227)
Submitted	7/27/2023 9:27:00 AM
Submitted by	Dr. Priya Vashisht
Submitter email	priya.vashisht@thapar.edu
Similarity	9%
Analysis address	priya.vashisht.thapar@analysis.urkund.com

Dr. Priya Vashisht

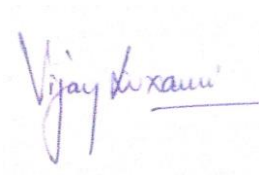

Dr. Vijay Luxami